NOAA Technical Report NESS 90

Total Precipitable Water and Rainfall Determinations from the Seasat Scanning Multichannel Microwave Radiometer (SMMR)

Washington, D.C. 20233
May 1982

U. S. DEPARTMENT OF COMMERCE
National Oceanic and Atmospheric Administration
National Earth Satellite Service

NOAA TECHNICAL REPORTS

National Earth Satellite Service Series

The National Earth Satellite Service (NESS) is responsible for the establishment and operation of the environmental satellite systems of NOAA.

Publication of a report in NOAA Technical Report NESS series will not preclude later publication in an expanded or modified form in scientific journals. NESS series of NOAA Technical Reports is a continuation of, and retains the consecutive numbering sequence of, the former series, ESSA Technical Report National Environmental Satellite Center (NESC), and of the earlier series, Weather Bureau Meteorological Satellite Laboratory (MSL) Report. Reports 1 through 39 are listed in publication NESC 56 of this series.

Reports in the series are available from the National Technical Information Service (NTIS), U.S. Department of Commerce, Sills Bldg., 5285 Port Royal Road, Springfield, VA 22161, in paper copy or microfiche form. Order by accession number, when given, in parentheses. Beginning with 64, printed copies of the reports, if available, can be ordered through the Superintendent of Documents, U.S. Government Printing Office, Washington, DC 20402. Prices given on request from the Superintendent of Documents or NTIS.

ESSA Technical Reports

NESC 46 Monthly and Seasonal Mean Global Charts of Brightness From ESSA 3 and ESSA 5 Digitized Pictures, February 1967-February 1968. V. Ray Taylor and Jay S. Winston, November 1968, 9 pp. plus 17 charts. (PB-180-717)

NESC 47 A Polynomial Representation of Carbon Dioxide and Water Vapor Transmission. William L. Smith, February 1969 (reprinted April 1971), 20 pp. (PB-183-296)

NESC 48 Statistical Estimation of the Atmosphere's Geopotential Height Distribution From Satellite Radiation Measurements. William L. Smith, February 1969, 29 pp. (PB-183-297)

NESC 49 Synoptic/Dynamic Diagnosis of a Developing Low-Level Cyclone and Its Satellite-Viewed Cloud Patterns. Harold J. Brodrick and E. Paul McClain, May 1969, 26 pp. (PB-184-612)

NESC 50 Estimating Maximum Wind Speed of Tropical Storms From High Resolution Infrared Data. L. F. Hubert, A. Timchalk, and S. Fritz, May 1969, 33 pp. (PB-184-611)

NESC 51 Application of Meteorological Satellite Data in Analysis and Forecasting. Ralph K. Anderson, Jerome P. Ashman, Fred Bittner, Golden R. Farr, Edward W. Ferguson, Vincent J. Oliver, Arthur H. Smith, James F. W. Purdom, and Rance W. Skidmore, March 1974 (reprint and revision of NESC 51, September 1969, and inclusion of Supplement, November 1971, and Supplement 2, March 1973), pp. 1--6C-18 plus references.

NESC 52 Data Reduction Processes for Spinning Flat-Plate Satellite-Borne Radiometers. Torrence H. MacDonald, July 1970, 37 pp. (COM-71-00132)

NESC 53 Archiving and Climatological Applications of Meteorological Satellite Data. John A. Leese, Arthur L. Booth, and Frederick A. Godshall, July 1970, pp. 1-1--5-8 plus references and appendixes A through D. (COM-71-00076)

NESC 54 Estimating Cloud Amount and Height From Satellite Infrared Radiation Data. P. Krishna Rao, July 1970, 11 pp. (PB-194-685)

NESC 56 Time-Longitude Sections of Tropical Cloudiness (December 1966-November 1967). J. M. Wallace, July 1970, 37 pp. (COM-71-00131)

NOAA Technical Reports

NESS 55 The Use of Satellite-Observed Cloud Patterns in Northern Hemisphere 500-mb Numerical Analysis. Roland E. Nagle and Christopher M. Hayden, April 1971, 25 pp. plus appendixes A, B, and C. (COM-73-50262)

NESS 57 Table of Scattering Function of Infrared Radiation for Water Clouds. Giichi Yamamoto, Masayuki Tanaka, and Shoji Asano, April 1971, 8 pp. plus tables. (COM-71-50312)

NESS 58 The Airborne ITPR Brassboard Experiment. W. L. Smith, D. T. Hilleary, E. C. Baldwin, W. Jacob, H. Jacobowitz, G. Nelson, S. Soules, and D. Q. Wark, March 1972, 74 pp. (COM-72-10557)

NESS 59 Temperature Sounding From Satellites. S. Fritz, D. Q. Wark, H. E. Fleming, W. L. Smith, H. Jacobowitz, D. T. Hilleary, and J. C. Alishouse, July 1972, 49 pp. (COM-72-50963)

NESS 60 Satellite Measurements of Aerosol Backscattered Radiation From the Nimbus F Earth Radiation Budget Experiment. H. Jacobowitz, W. L. Smith, and A. J. Drummond, August 1972, 9 pp. (COM-72-51031)

(Continued on inside back cover)

NOAA Technical Report NESS 90

Total Precipitable Water and Rainfall Determinations from the Seasat Scanning Multichannel Microwave Radiometer (SMMR)

John C. Alishouse

Washington, D.C. 20233
May 1982

U. S. DEPARTMENT OF COMMERCE
Malcolm Baldrige, Secretary

National Oceanic and Atmospheric Administration
John Byrne, Administrator

National Earth Satellite Service
John H. McElory, Assistant Administrator for Satellites

CONTENTS

FIGURES

TABLES

TOTAL PRECIPITABLE WATER AND RAINFALL DETERMINATIONS FROM THE SEASAT SCANNING MULTICHANNEL MICROWAVE RADIOMETER (SMMR)

John C. Alishouse
National Earth Satellite Service, NOAA
Washington, D.C. 20233

ABSTRACT. Three of the SEASAT SMMR's five frequencies can be used to determine the total precipitable water in the atmosphere, the liquid water content, and the rainfall rate. In addition two distinct algorithms were used to derive geophysical parameters from brightness temperature. Comparisons with surface observations from the Gulf of Alaska SEASAT Experiment (GOASEX) and with other selected sources were made for both algorithms. Generally, very good agreement was found between satellite and radiosonde observations of total precipitable water. An estimate of the precision of radiosonde derived total precipitable water amounts was made. Comparisons of precipitation occurrence as determined from the SMMR and surface observations also were made. In the tropics, very good agreement is found between satellite and surface observations. In the midlatitudes (Gulf of Alaska) it is found that small cells of precipitation are often missed by the SMMR, but larger synoptic scale precipitation is detected. Raob tabulations and corrections, listings of computer programs, and raob precision statistics are given in appendixes A, B, and C.

INTRODUCTION

SEASAT, the first satellite devoted primarily to oceanography, was launched on June 28, 1978, and ceased operation on October 10, 1978. SEASAT carried a complement of four microwave sensors and one visible/infrared sensor (Born et al., 1979). One of the sensors was the Scanning Multichannel Microwave Radiometer (SMMR) (Gloersen and Barath, 1977). The SMMR has the capability of measuring a number of geophysical parameters. The 1.7-, 1.4-, and 0.81-cm channels may be used to infer the total precipitable water, liquid water content, and rainfall rate. It has been possible to verify the accuracy of the SMMR's total precipitable water determinations by comparisons with values obtained from radiosondes from the small island weather stations, Ocean Weather Stations Papa and Tango, and the R/V Oceanographer. Enough surface observations of rainfall are available so that, at least, a verification of precipitation detection has been possible. It was not possible to verify the liquid water content values derived from the SMMR data.

Two distinct algorithms were used to derive the geophysical parameters. One is a regression algorithm that has the form $\sum_i \sum_j \ln(280-T_{Bij})$, where the subscripts i and j refer to wavelength and polarization state. Originally, the a_{ij}'s were derived by Wilheit and Chang (Wilheit and Chang, 1979) from brightness temperatures computed from a wide range of geophysical conditions. Subsequently, as SMMR data became available, this algorithm was modified by T. Chester (SEASAT, 1980a and 1981) to account for observed biases and other deviations. In the course of the SEASAT data reduction, this algorithm was first called the Wilheit algorithm and later the Chester algorithm. Throughout this report it will be referred to as the regression algorithm. The other algorithm is a nonlinear, least-squares, iterative, estimation algorithm (Bierman et al., 1978). This algorithm minimizes the mean square difference between a set of computed and measured brightness temperatures. The brightness temperatures are computed from a model function (Wentz, 1982) with the appropriate geophysical inputs. Like the regression algorithm, biases were removed and adjustments were made as real data became available. This algorithm is often called the Wentz algorithm. Throughout this report, it will be referred to as the estimation algorithm.

A series of special measurements was made in the northwest Pacific and Gulf of Alaska during August and September, 1978. This data gathering effort, called the Gulf of Alaska Seasat Experiment (GOASEX), was an intensive effort to collect surface measurements that could be used to verify the SEASAT experiments. Included in the GOASEX measurements (Wilkerson et al., 1979) was a series of special radiosonde ascensions from ocean weather station Papa and the NOAA R/V Oceanographer.

At the GOASEX I Workshop (SEASAT, 1979a), there appeared to be a correlation between sea surface temperature deviation from surface truth and atmospheric precipitable water content for the estimation algorithm. A possible explanation was that the water vapor attenuation correction was being improperly applied. The amount of water vapor calculated by both the estimation and regression algorithms was in fairly good agreement with the five available radiosondes from ocean weather station Papa and the R/V Oceanographer. These five soundings, however, did not represent a wide range of atmospheric precipitable water. To obtain a wider range of values, it was decided to look at tropical stations. Because of the contamination of SMMR data by the presence of land, only stations on small atolls would be useful.

At the SMMR Mini-Workshop I (SEASAT, 1979b), it was noted that, for the available observations from tropical radiosondes, the satellite estimates were about 20 percent high. Between Mini-Workshop I and Mini-Workshop II (SEASAT, 1979c), an improved antenna pattern correction algorithm and additional calibration corrections were introduced into the SMMR data processing. This permitted the computation of more accurate brightness temperatures and hopefully more accurate geophysical parameters. In addition, more radiosondes from other tropical island stations were obtained.

At the SMMR Mini-Workshop II, it was found that the estimation algorithm produced results that were underestimates of 2.7 percent in the GOASEX region and overestimates of 21 percent in the tropics. The regression algorithm produced consistent overestimates of about 17 percent in both the GOASEX region and the tropics. Between SMMR Mini-Workshop II and SMMR Mini-Workshop III (SEASAT, 1980a), considerable SMMR data were processed. For the first time since the evaluation began, it was possible to compare statistically significant sample sizes. Also, the algorithms themselves seemed to have entered a period of tranquility. It was found that the estimation algorithm produced a slight overestimation in the GOASEX region and a slight underestimate in the tropics. It was also found that the estimation algorithm had a mean square error of 11 percent for GOASEX and 8 percent for the tropics. The regression algorithm was found to have a negative bias (overestimate) of 8 percent in the tropics. With an expanded data base both algorithms were tuned to eliminate some of the problems revealed in Mini-Workshop III. At SMMR Mini-Workshop IV (SEASAT, 1981) "final" versions of the algorithms were used in the computation of the geophysical parameters. These results are the ones that will be presented in this report.

SELECTION OF STATIONS AND ORBITS

The R/V Oceanographer and Ocean Station Papa made special radiosonde ascensions that were coincident with SEASAT overpasses. In the selection of tropical radiosondes to compare with SEASATderived values, additional factors were involved. It was necessary to determine overpass times and whether the island on which the radiosonde station was located was sufficiently large to affect the water vapor determination. The overpasses and their times were determined utilizing the Seatrak calculator and a JPL computer program. Table 1 is a listing of the possible stations.

During GOASEX, SEASAT was in a 3-day, 43-revolution repeat cycle. It was found that certain sets of revolutions passed over more radiosonde stations than others. The most fruitful set was found to pass directly over Wake Island, Majuro, and Funafuti and very nearly over Kwajalein and Nandi, Fiji. This set corresponded to the end of one revolution and the beginning of another. Radiosonde data from these islands were collected and tabulated for revolutions 1085-6 on September 10 through revolutions 1386-7 on October 1. Another set of revolutions passed directly over Truk, Kapangamarangi, and very nearly over Ponape. Radiosonde data from Truk and Ponape were collected and tabulated

for revolution 1101 on September 11 through 1402 on October 3. A third set of revolutions passed over Guam, Woleai, and Ocean Station Tango. Radiosonde data from Guam and Tango were collected and tabulated for revolution 1087 on September 10, through revolution 1388 on October 2. All processed radiosondes for the GOASEX time frame are listed in appendix A. These tables list the total precipitable water in gm/cm^2, the date and time of the radiosonde ascension, and the applicable SEASAT revolution number.

Table 1. Possible raob stations

Station	Lat.	Long.[1]	Area (km^2)	Percent of retrieval grid[2]	Comments
Tango	29 N	135	-	-	weather ship
Midway	28.22N	182.63	15	0.5	sta. elevation = 111 m
Guam	13.55N	144.83	541	19	
Wake Island	19.28N	166.65	8	0.3	
Eniwetok	11.35N	162.35			
Johnston Is.	16.73N	190.48	1.3	.04	
Woleai	7.38N	143.92			
Truk	7.47N	151.85	118	4.0	
Ponape	6.87N	158.22	455	16	
Kwajalein	8.72N	167.73	16	0.5	
Majuro	7.03N	171.38	10	0.3	
Koror	7.33N	134.48	8	0.3	
Yap	9.48N	138.08	54	1.9	
Kapangamarangi	1.08N	154.77	<76	<2.6	
Tarawa	13.05N	172.92	23	0.8	
Honiara	9.42S	159.97	6475	222	on Guadalcanal Is.
Vila	17.75S	168.30	915	31	on Efate Is. in New Hebrides
Noumea	22.27S	166.45	19,099	655	on New Caledonia
Funafuti	8.52S	179.22	2.8	0.1	
Nandi	17.75S	177.46	10,386	356	On Vita Levu Is. in Fiji Islands
Canton Island	2.77S	188.28	9	0.3	
Pago Pago	14.33S	189.28	135	4.6	on Tutuila Is. in American Samoa
Penrhyn	9.02S	201.93	10	0.3	
Atuoma	9.82S	220.98	200	6.9	on Hiva Oa Is. in Marquises Isles in French Polynesia
Tahiti	17.55S	210.38	1042	36	
Tuamotu	18.07S	219.05			on Hao Island

[1]Longitudes are expressed as east longitudes conforming to SEASAT Project practice.

[2]Precipitable water is retrieved on a 54 x 54 km grid. For this comparison, the grid was assumed to be square.

RADIOSONDE DATA PROCESSING

The radiosonde data were received in a wide variety of formats, which required some flexibility in handling the data. The data were screened for superadiabatic lapse rates and supersaturation, the exact screening being a function of the particular format of the radiosonde data. "Slightly" superadiabatic lapse rates were ignored, while soundings with "grossly" superadiabatic lapse rates were plotted and corrected if possible. All soundings with supersaturated water vapor concentrations were rejected. The variety of formats for the radiosonde data required two distinct computer programs for the processing of the data. (These programs are given in appendix B.) One program used moisture data in terms of relative humidity and the other program used dew point depression. The preferred format was the relative humidity as this is the primary measurement of the humidity sensing element; however, dew point depression is usually transmitted. Tetens' formula (Tetens, 1930) was used to compute the vapor pressure:

$$e_I = 6.11 \exp. [17.27\, T_D/(237.3 + T_D)],$$

where e_I = vapor pressure in mb and
T_D = dew point temperature in °C.

The mixing ratio is then calculated from the expression,

$$q = \frac{621.98 e_I}{P - e_I} \text{ g/kg},$$

where P = pressure in mb

When the humidity data are expressed as relative humidity, the equations become

$$e_w = 6.11 \exp. [17.27\, T_A/(237.3 + T_A)]$$

and $$e_I = e_W \frac{RH}{100},$$

where T_A = air temperature in °C,
e_w = saturation vapor pressure in mb, and
RH = relative humidity in percent.

The mixing ratio is calculated as before. The total precipitable water is then calculated using the expression,

$$U = \frac{1}{g} \int_{P_o}^{\infty} q\,(P)\, dp,$$

where P_o = surface pressure

This integral is done as a summation utilizing the trapezoidal rule

$U = \frac{1}{2g} \Sigma (q_i + q_{i+1})(P_i - P_{i+1})$. The number of quadrature points varied with the particular radiosonde. As a general rule, all significant levels were used and almost all the mandatory levels also were used even though these are sometimes interpolated values. The radiosondes from the R/V Oceanographer were processed by NOAA's Pacific Marine Environmental Laboratories (PMEL).

Most of the radiosonde humidity measurements terminate at about 300 mb. Based on climatological data, it was decided that corrections for water vapor above this level were not necessary. In the case of Ocean Station Papa, the radiosonde data were available only to 400 mb. In the case of the Oceanographer, the maximum height achieved was often less than 300 mb. A correction based on midlatitude climatology was devised. The details of the corrections are given in appendix A. The Guam radiosonde station is located 111 m above sea level. The Guam total water vapor values were corrected to sea level by assuming this layer was the same temperature and had the same mixing ratio as the Guam surface values. This amounted to a correction of 0.2 gm/cm^2 in all cases.

SATELLITE RESULTS

Total Precipitable Water Determinations

Two previous satellite experiments, the Nimbus E Microwave Spectrometer (NEMS) on Nimbus 5 and Scanning Microwave Spectrometer (SCAMS) on Nimbus 6, were capable of making total precipitable water measurements. Results from the NEMS were published by Staelin et al. (1976), and results from the SCAMS were published by Grody et al. (1980). The present SMMR differs from the previous experiments in that it uses three wavelengths (1.7-, 1.4-, and 0.81-cm) as compared with two wavelengths (1.35-and 0.95-cm) used in the NEMS and SCAMS experiments. The SMMR water vapor retrievals are on a 54 x 54 km grid, whereas the NEMS and SCAMS retrievals are on a 250 x 250 km grid. The inversion algorithms used on the NEMS and SCAMS data were regression algorithms. Cosmos 243 carried a five-channel radiometer that permitted the determination of total precipitable water utilizing its 1.35-and 0.8-cm channels. Results from this experiment were published by Gurvich and Demin (1970). Results from the Nimbus 7 SMMR were published by Prabhakara et al (1981).

Two data sets were employed in this comparison. The first data set comes from Ocean Station Papa and the R/V Oceanographer. This is the GOASEX or mid-latitude data set. The second is from the tropics. Separate comparisons have been made for each of the two algorithms. To be considered in the statistics, it was required that the radiosonde ascension and satellite overpasses be coincident within $\pm$ 2 hours and $\pm$ 1° in latitude and longitude. Precipitation was screened using the algorithm's determination and not the surface observations. Table 2 presents the matchups from the tropics for comparison with the regression and estimation algorithms. Table 3 presents the matchups for the GOASEX data set. The time is approximately the time of the satellite overpass.

Precipitation events were excluded from the initial evaluation as neither algorithm was designed to retrieve total precipitable water in the presence of rain. Additionally, it was desired to see if there were any biases associated with the amount of total precipitable water. This was investigated by analyzing the tropical and GOASEX data sets separately. Thus, the initial evaluation was done on data sets that were separated geographically and from which precipitation events were eliminated. The determination of precipitation was from the algorithms themselves. Table 4 presents statistics from the tropics for both the regression and estimation algorithm.

Table 2. Tropical data

				Estimation Algorithm		Regression Algorithm	
Station	Rev	Time(Z)	Raob	SMMR	Rain	SMMR	Rain
Funafuti	1086	22:16:14	4.7	4.3	No	4.3	Yes
Majuro	1086	22:20:45	4.5	4.6	No	4.6	No
Kwajalein	1086	22:20:45	5.5	5.4	Yes	5.4	Yes
Wake Island	1086	22:23:46	5.0	5.2	No	5.1	No
Funafuti	1129	22:27:43	3.8	3.9	No	3.7	No
Majuro	1129	22:33:43	6.2	5.6	Yes	6.1	Yes
Kwajalein	1129	22:33:43	5.6	5.7	No	5.7	No
Wake Island	1129	22:36:44	5.3	4.6	Yes	5.4	Yes
Funafuti	1172	22:40:48	3.2	3.6	No	3.6	No
Majuro	1172	22:45:19	6.1	5.6	Yes	5.8	Yes
Kwajalein	1172	22:46:49	5.1	5.1	No	5.2	No
Wake Island	1172	22:49:51	3.6	4.0	No	3.8	No
Funafuti	1215	22:53:13	3.7	4.1	No	-	-
Majuro	1215	22:59:14	5.0	5.5	No	-	-
Kwajalein	1215	22:59:14	6.6	5.8	Yes	-	-
Wake Island	1215	23:02:15	4.2	4.5	No	-	-
Funafuti	1258	23:07:13	6.4	6.1	No	6.1	Yes
Funafuti	1301	23:18:44	5.1	4.6	No	4.5	No
Majuro	1301	23:24:45	5.2	5.3	No	5.4	No
Funafuti	1344	23:31:43	5.4	5.9	No	5.6	Yes
Majuro	1344	23:36:13	5.5	5.4	No	5.4	No
Kwajalein	1344	23:37:44	5.0	5.4	No	5.4	No
Wake Island	1344	23:40:44	5.5	5.4	No	5.3	No
Funafuti	1387	23:44:44	6.3	5.8	No	5.8	Yes
Majuro	1387	23:49:15	4.6	4.9	No	5.4	No
Kwajalein	1387	23:50:45	5.3	5.2	No	5.2	No
Wake Island	1387	23:53:46	4.7	4.8	No	4.7	No

Table 2. Tropical data continued

Station	Rev	Time(Z)	Raob	Estimation Algorithm SMMR	Estimation Algorithm Rain	Regression Algorithm SMMR	Regression Algorithm Rain
Guam	1130	0:15:43	5.4	5.7	Yes	5.8	No
Tango	1130	0:20:14	4.0	4.4	No	4.1	No
Guam	1173	0:28:45	5.0	5.4	Yes	5.5	Yes
Tango	1173	0:33:16	4.7	4.4	No	4.2	No
Guam	1216	0:41:31	5.1	5.3	Yes	-	-
Guam	1259	0:53:43	5.9	5.7	Yes	6.0	Yes
Tango	1259	0:58:14	5.8	5.8	Yes	5.9	Yes
Guam	1302	1:06:45	5.0	5.5	Yes	6.3	Yes
Tango	1302	1:11:16	3.5	3.3	No	3.1	No
Guam	1302	1:06:45	5.0	5.5	Yes	5.6	Yes
Tango	1302	1:11:16	3.5	3.3	No	3.1	No
Guam	1345	1:19:44	6.0	6.0	Yes	6.3	Yes
Tango	1345	1:24:14	4.1	3.9	No	3.6	No
Guam	1388	1:31:44	5.2	6.0	Yes	6.2	Yes
Truk	1101	23:31:42	5.3	5.0	No	5.1	No
Ponape	1101	23:31:42	4.9	5.9	No	6.2	Yes
Truk	1144	23:44:44	6.0	5.6	No	5.9	No
Ponape	1144	23:44:44	6.0	5.8	No	5.8	No
Truk	1273	0:22:45	6.3	5.6	Yes	6.0	Yes
Ponape	1273	0:22:45	5.2	5.5	No	5.6	No
Truk	1316	0:35:42	5.1	5.0	No	5.2	No
Ponape	1316	0:35:42	5.7	5.8	No	6.1	No
Truk	1359	0:48:44	6.4	5.7	Yes	6.2	Yes
Truk	1402	1:00:45	5.9	5.7	No	6.1	No
Ponape	1402	1:00:45	5.8	5.8	No	6.1	No

Table 3. GOASEX data

Station	Rev	Time(Z)	Raob	Estimation Algorithm SMMR	Estimation Algorithm Rain	Regression Algorithm SMMR	Regression Algorithm Rain
Ocean	940	17:23:41	1.8	2.2	No	2.1	No
Papa	940	17:23:41	1.9	2.1	No	2.1	No
Papa	963	8:20:43	1.6	1.7	No	1.7	No
Papa	977	7:52:40	1.4	1.6	No	1.5	No
Papa	983	17:35:42	1.6	1.8	No	-	-
Papa	1006	8:32:43	2.9	3.2	No	2.7	No
Papa	1020	8:04:41	3.7	4.4	No	3.8	Yes
Papa	1049	8:45:08	2.0	-	-	2.0	No
Ocean	1063	8:17:06	1.6	-	-	1.6	No
Ocean	1069	17:59:44	1.5	1.6	No	-	-
Ocean	1106	8:29:43	1.5	1.7	No	1.5	No
Papa	1106	8:29:43	1.8	1.9	No	1.7	No
Ocean	1120	8:00:44	1.6	1.5	No	1.4	No
Papa	1135	9:10:44	1.2	1.3	No	1.3	No
Ocean	1149	18:42:41	1.3	1.3	No	1.2	No
Papa	1149	18:42:41	1.2	1.3	No	1.2	No
Ocean	1155	18:24:42	1.9	1.5	No	1.4	No
Papa	1155	18:24:42	1.4	1.2	No	1.3	No
Ocean	1163	8:13:42	1.2	1.3	No	1.1	No
Papa	1178	9:23:41	1.3	1.5	No	1.4	No
Ocean	1192	8:56:12	3.4	4.3	Yes	3.6	Yes
Papa	1192	8:54:42	2.6	3.2	No	2.6	No
Papa	1198	18:38:41	3.5	4.4	No	3.5	No
Papa	1221	9:37:12	1.6	1.7	No	1.5	No
Papa	1241	18:51:43	1.1	1.3	No	1.3	No
Ocean	1249	8:38:40	1.3	1.2	No	1.1	No
Papa	1264	9:48:40	1.2	1.1	No	1.1	No

Table 3. GOASEX data continued

Station	Rev	Time(Z)	Raob	Estimation Algorithm SMMR	Estimation Algorithm Rain	Regression Algorithm SMMR	Regression Algorithm Rain
Papa	1278	9:29:42	1.1	1.0	No	1.0	No
Papa	1284	19:03:44	1.3	1.2	No	1.2	No
Ocean	1292	8:51:08	2.2	2.7	No	2.4	No
Papa	1307	10:00:36	2.5	-	-	2.4	Yes

Table 4. Tropical statistics (nonprecipitating)

Regression algorithm

n = no. of obs. = 30

Raob Mean = 5.0 gm/cm^2 std dev = 0.8 gm/cm^2 = 16 percent

bias = Raob - SMMR = 0.007 gm/cm^2

Mean square error = $\left[\frac{\Sigma(R_i-S_i)^2}{n}\right]^{\frac{1}{2}}$ where R_i = ith radiosonde

S_i = corresponding satellite value

m.s.e. = 0.3 gm/cm^2

Estimation algorithm

n = 35

Raob Mean = 5.0 gm/cm^2 std dev = 0.8 gm/cm^2

bias = 0.05 gm/cm^2 m.s.e. = 0.3 gm/cm^2

Thus we see there is good agreement between surface and satellite observations for both algorithms in the tropics in non-precipitating situations.

In examining the tropical data, it was noted that a number of the events that were excluded were of light rain (i.e. <1 mm/hr) and also that there were a reasonable number of such events. Table 5 presents statistics from the tropics for precipitating cases.

Table 5 - Tropical Statistics (precipitating)

Regression Algorithm

n = 15, Raob Mean = 5.7 gm/cm^2 bias = -0.2 gm/cm^2

std dev = 0.54 gm/cm^2

m.s.e. = 0.5 gm/cm^2

Estimation Algorithm

n = 15, Raob Mean = 5.7 gm/cm^2, bias = 0.14 gm/cm^2, std dev = 0.54 gm/cm^2

m.s.e. = 0.5 gm/cm^2

While the mean square error is a reasonable value (9 percent), we note it is almost the same as the standard deviation of the raob sample set. Eliminating the bias does not significantly reduce the error.

Table 6 presents the GOASEX results for nonprecipitating cases.

Table 6. GOASEX statistics (nonprecipitating)

Regression Algorithm

n = 26 Raob Mean = 1.7 gm/cm^2 bias = 0.03 gm/cm^2

std dev = 0.6 gm/cm^2

m.s.e. = 0.16 gm/cm^2

Estimation Algorithm

n = 27 Raob Mean = 1.9 gm/cm^2, std dev = 0.7 gm/cm^2

bias = -0.16 gm/cm^2 m.s.e. = 0.32 gm/cm^2

m.s.e.(with bias removed) = 0.28 gm/cm^2

A statistically significant number of precipitation events are not available from the GOASEX data set, so precipitation statistics have not been computed for the GOASEX data.

The regression algorithm (figure 1) shows a negligible bias and an error of less than 10 percent, whereas the natural variance of the sample set is 35 percent. The estimation algorithm shows a tendency to overestimate in the GOASEX area, although a closer examination of the data shows most of the bias comes from overestimations of large (for the GOASEX area) amounts of water vapor. These cases are clearly evident in figure 2.

Figure 1 plots raob (abscissa) vs satellite (ordinate) determinations of total precipitable water for the regression algorithm and shows uniformly good agreement between satellite and surface observations. Figure 2 is a plot of raob (abscissa) vs satellite (ordinate) for the estimation algorithm. The estimation algorithm appears to work well at the extremes (small and large amounts of total precipitable water) but shows a distinct tendency towards overestimation in the mid-range values, especially in the GOASEX data set. Some of these GOASEX events are associated with precipitation as determined from surface observations.

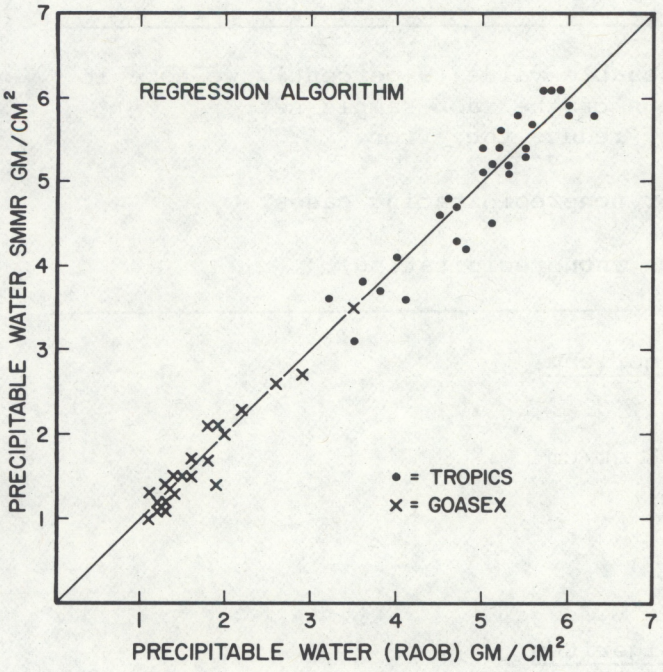

Figure 1.--Precipitable water in gm/cm^2 as determined from radiosonde observations (raobs) vs SMMR determinations by the regression algorithm.

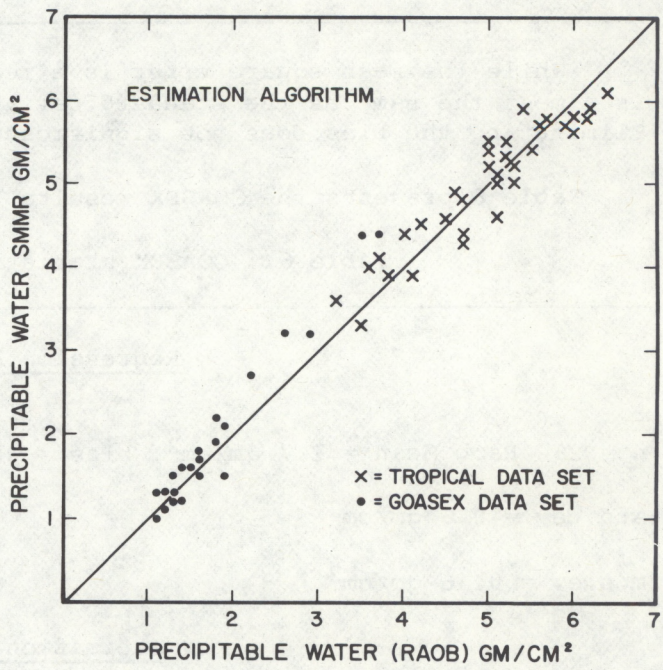

Figure 2.--Precipitable water in gm/cm^2 as determined from raobs vs SMMR determinations by the estimation algorithm.

Time Series for Ocean Weather Station Papa

Figures 3 and 4 are a time series for ocean weather station Papa ranging from August 31, 1978, (DOY 243) to September 26, 1978, (DOY 269). The abscissa is the time scale in Julian days. The left ordinate is the total precipitable water in gm/cm^2 and applies to both the radiosonde and SMMR values. The right ordinate refers to the liquid water content of the atmosphere and pertains only to the SMMR data as no surface observations of liquid water content were made.

The large amounts of water vapor observed on days 249 and 261 correspond to frontal passages. These frontal passages show the tendency of the estimation algorithm to overestimate the water vapor as the water vapor amount increases. These figures also show the difficulties in detecting the presence of precipitation using either algorithm.

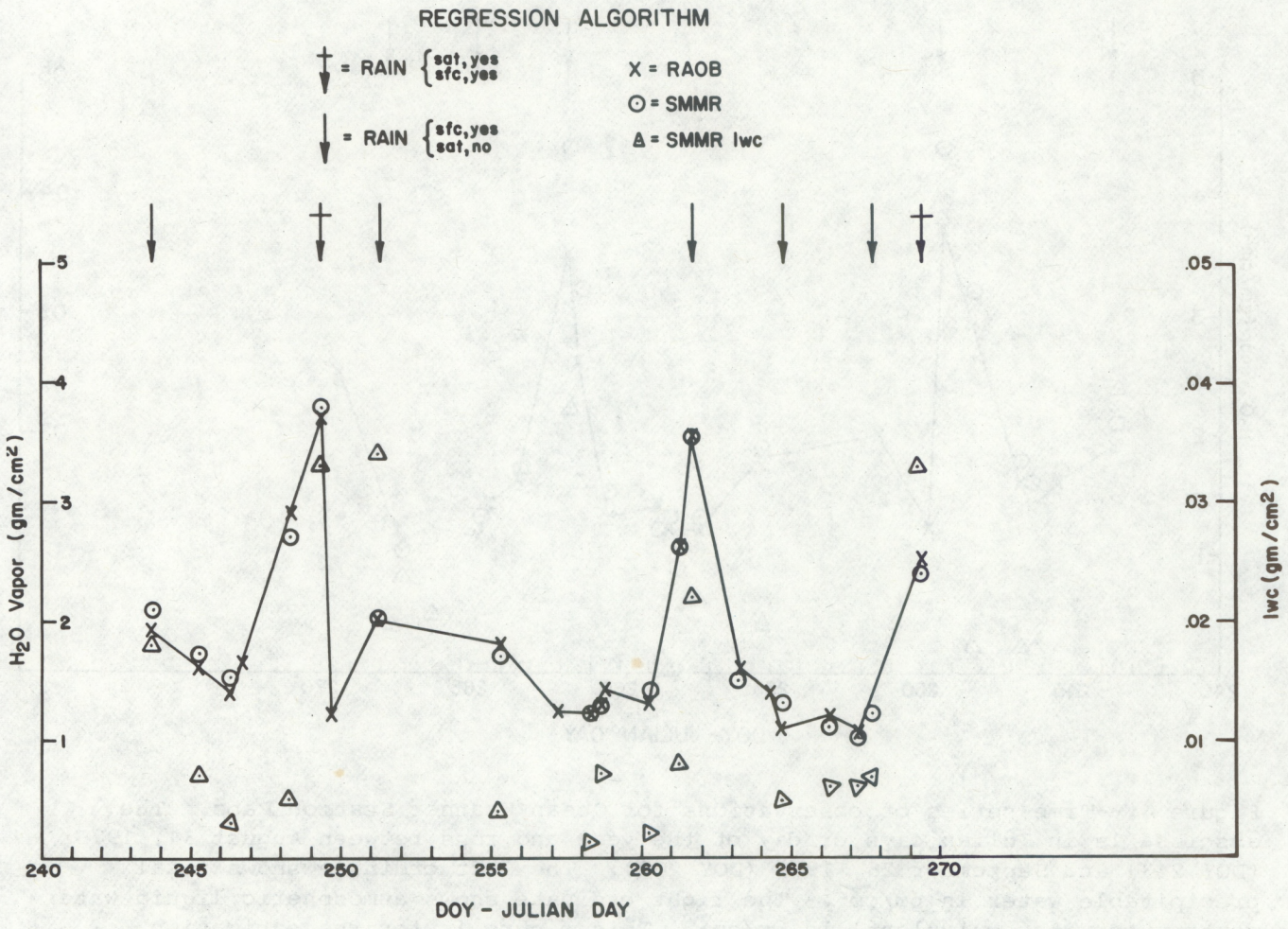

Figure 3.--Time series of obsrvations for Ocean Weather Station Papa. The abscissa is in Julian days or day of the year and runs between August 11, 1978 (DOY 243) and September 26, 1978 (DOY 269). The left ordinate shows total precipitable water in gm/cm^2. The right ordinate shows atmospheric liquid water content in gm/cm^2 . This figure is for the regression algorithm.

ERROR ANALYSIS

Figures 5 and 6 are error histograms for the regression and estimation algorithms, respectively. The two data sets (tropical and GOASEX) have been combined in these figures. The solid lines represent the observed number of errors and the dashed lines the expected (assuming a normal distribution) number. Both sets of error statistics can be fit by a normal distribution as evidenced by the chi-squared values.

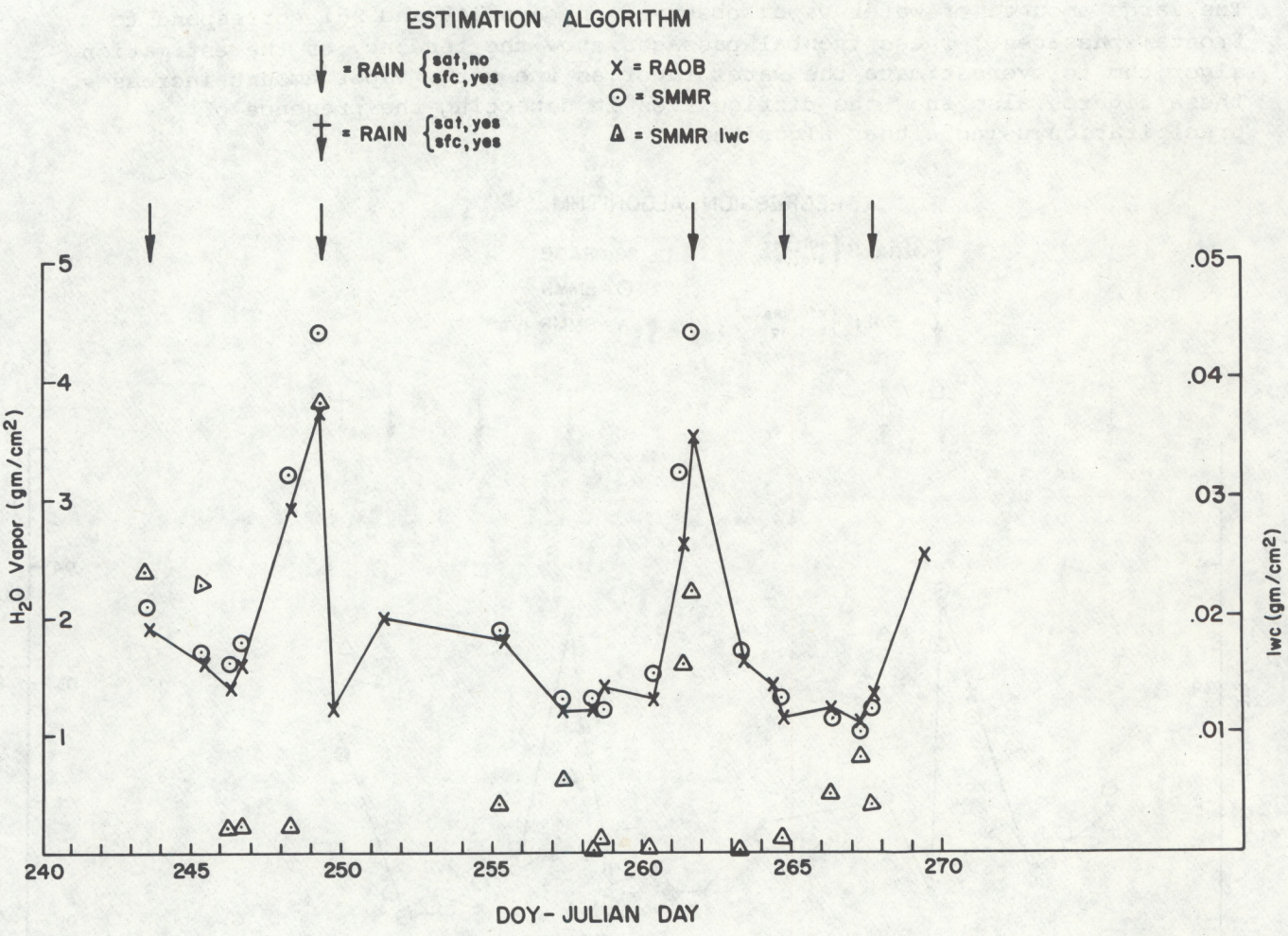

Figure 4.--Time series of observations for Ocean Weather Station Papa. The abscissa is in Julian days or day of the year and runs between August 31, 1978 (DOY 243) and September 26, 1978 (DOY 269). The left ordinate shows total precipitable water in gm/cm^2. The right ordinate shows atmospheric liquid water content (or its equivalent) in gm/cm^2. This figure is for the estimation algorithm.

An important part of any comparison of measurements is the accuracy of the individual measurements that are being used as standards. In this case, we are using the radiosonde as a standard and determining the acuracy of the satellite instrument relative to the radiosonde. A series of measurements (Hoehne, 1980) were made to assess the functional precision of radiosondes. These measurements consisted of a series of 50 ascensions carrying two radiosondes. The operational sonde was mounted 5m below the test sonde. The sondes are powered by water actuated batteries; thus, the operational sonde passes through some of the water emitted by the test sonde's batteries. This reuslts in a small but statistically significant bias. These radiosonde data were obtained, and the total precipitable water for each radiosonde was calculated. Using standard statistical techniques, a coefficient of variance of 0.042 for an individual raob was established. This data set and details of the analysis are presented in appendix C. Applying this coefficient of variance to tropical and GOASEX data sets, estimates of the precision of the SMMR and radiosonde were made. Tables 7 and 8 present the results for the regression algorithm and estimation algorithm, respectively.

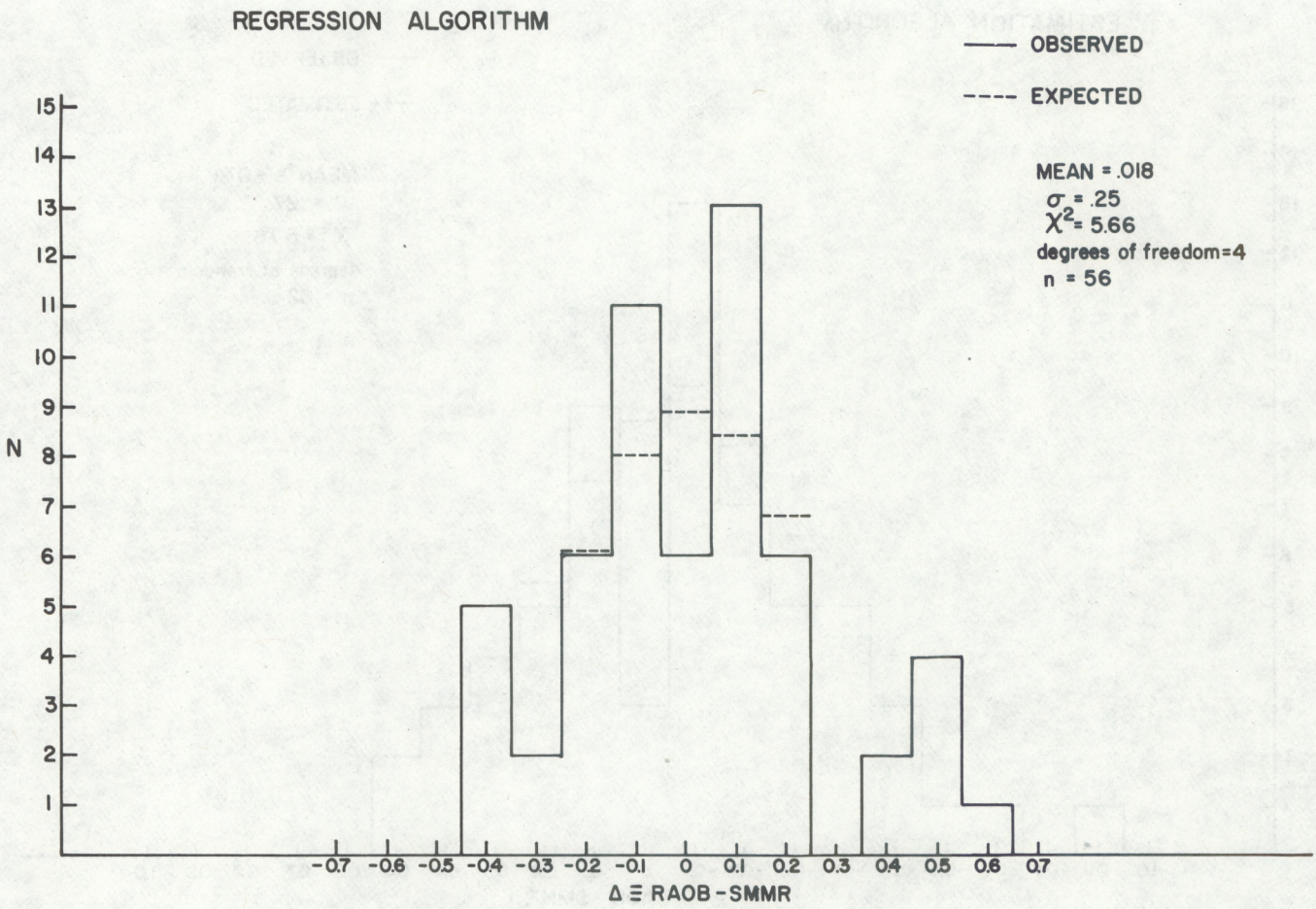

Figure 5.--Error historgram for the regression algorithm. The abscissa shows Δ, the difference between the raob and the SMMR. The ordinate shows the number of differences in each interval of 0.1 gm/cm^2. The interval centers are indicated on the abscissa.

Table 7. Raob and SMMR precisions (regression algorithm)

GOASEX data		Tropical data	
Sample Mean (raobs)	= 1.7 gm/cm^2	Sample Mean (raobs)	= 5.0 gm/cm^2
Raob precision	= 0.07 gm/cm^2	Raob precision	= 0.21 gm/cm^2
SMMR precision	= 0.14 gm/cm^2	SMMR precision	= 0.21 gm/cm^2

Table 8. Raob and SMMR precisions (estimation algorithm)

GOASEX data		Tropical data	
Sample Mean (raobs)	= 1.9 gm/cm^2	Sample Mean (raobs)	= 5.0 gm/cm^2
Raob precision	= 0.08 gm/cm^2	Raob precision	= 0.21 gm/cm^2
SMMR precision	= 0.27 gm/cm^2	SMMR precision	= 0.21 gm/cm^2

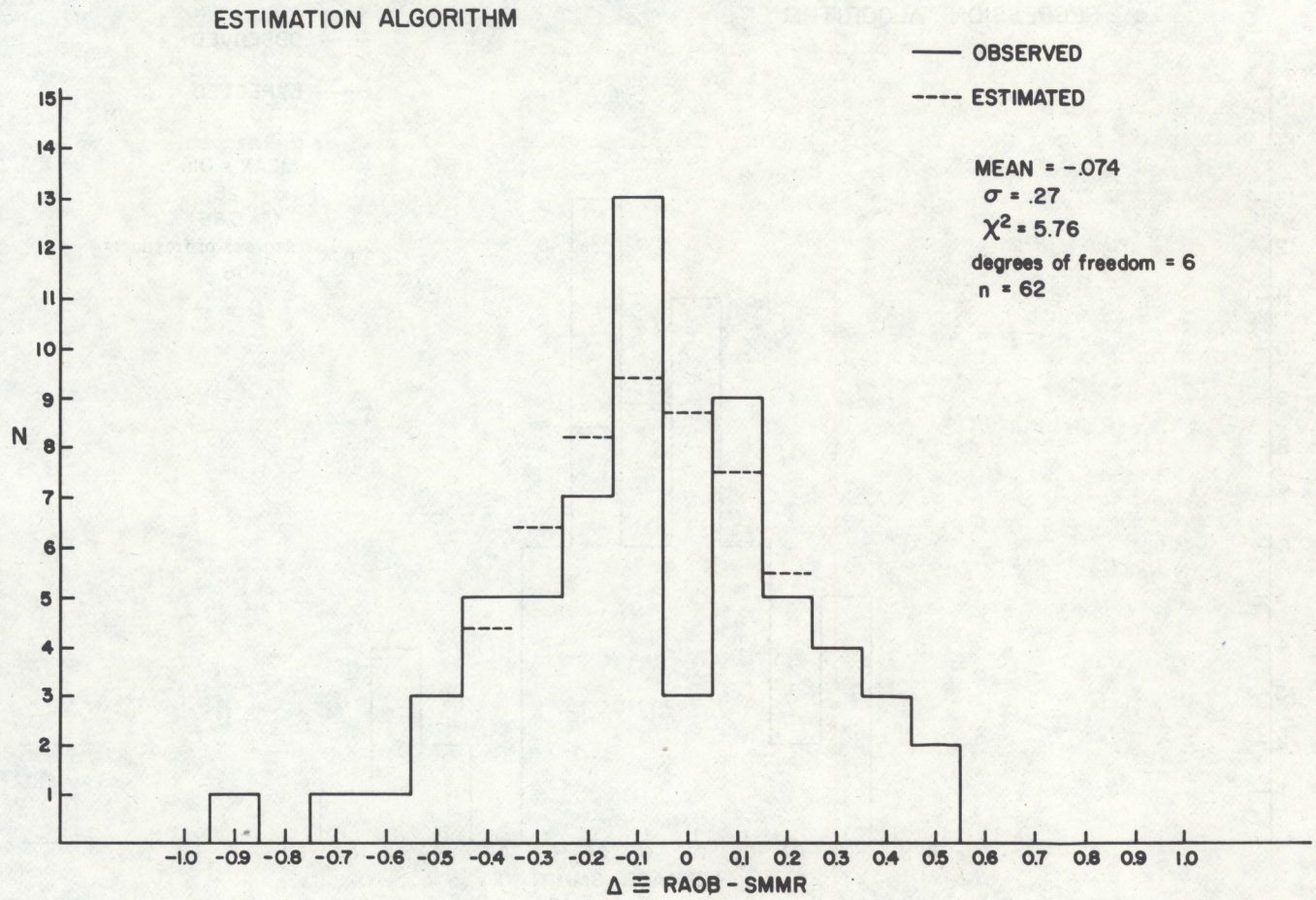

Figure 6.--Error histogram for the estimation algorithm. The abscissa shows Δ, the difference between the raob and the SMMR. The ordinate shows the number of differences in each interval of 0.1 gm/cm^2. The interval centers are indicated on the abscissa.

In the tropics, total precipitable water can be inferred from the SMMR by either algorithm with as much precision as from raobs. This is of particular significance in view of the paucity of surface observations from the tropics. In the midlatitudes, the SMMR's precision is less than that of raobs; but the regression algorithm's precision of 0.14 gm/cm^2 is well within the 0.2 gm/cm^2 goal of the experiment. The estimation algorithm's difficulties with the GOASEX data have been discussed previously.

RAINFALL COMPARISONS

Although the SMMR algorithms derive rainfall rate (mm/hr), the nature of the available surface observations made it impossible to determine a comparable rate. Therefore, the comparisons were made on a simple "yes or no " basis. Even this information is of value over the ocean where little data about precipitation are available. The surface determinations are based mainly on the 0Z or 12Z surface report. If there was doubt after the teletype message, and the station in question was a U.S. station, then the hourly surface observations (NOAA Form, MF1-10A) were obtained. This additional data usually permitted the definite assignment of "raining" or "not raining" at the satellite overpass time.

Table 9 shows the results for the tropical data set. The first entry in the table shows that there were five cases for which the SMMR indicated the presence of rain, and the surface observations confirmed this. The second entry shows that there were 13 cases for the regression algorithm and 15 cases for the estimation algorithm for which both the SMMR data and surface observations indicated no precipitation. Both algorithms correctly infer the pesence of rain in five of six cases of actual rain. In the tropics, the SMMR appears to be a reliable indicator of precipitation.

Table 10 shows the same type of results from GOASEX. The classification, surface, no; satellite, yes, is not shown in tables 9 and 10. With a few exceptions involving both algorithms and passes over Guam, this classification was not observed. The Guam cases are believed to be related to the size of Guam. It fills almost 20 percent of the 54 km x 54 km retrieval grid. The

Table 9. Tropical rainfall determinations

Surface, yes Satellite, yes	Regression 5 Estimation 5
Surface, no Satellite, no	Regression 13 Estimation 15
Surface, yes Satellite, no	Regression 1 Estimation 1
	Regression 18/19 Estimation 20/21
Actual Rain	Regression 5/6 Estimation 5/6

Table 10. GOASEX rainfall determinations

Surface, yes Satellite, yes	Regression 3 Estimation 1
Surface, no Satellite, no	Regression 15 Estimation 19
Surface, yes Satellite, no	Regression 5 Estimation 5
	Regression 18/23 Estimation 20/25
Actual Rain	Regression 3/8 Estimation 1/6

GOASEX surface results come from special observations taken by Ocean Weather Station Papa and the NOAA R/V Oceanographer at the time of the SEASAT overpasses. On an overall basis, both algorithms give good agreement between surface observations and satellite retrievals. Most of the agreements come from no-rain cases. In the tropics, both algorithms seem to be reliable indicators of rain. In the midlatitudes, both algorithms underestimate the occurrence of rain: three of eight and one of six for the regression and estimation algorithms, respectively. Similar results have been obtained in the JASIN* experiment (SEASAT, 1980b). A number of factors can be cited for the underestimates. A number of the cases in the GOASEX comparisons were of light rain. Because of the lower tropopause height and freezing level in the midlatitudes, it is likely that the midlatitude precipitation events contain less liquid water than the tropical ones. The slightly higher success rate of the regression algorithm is probably explained by its use of the full resolution (27 x 27 km) of the 0.81-cm channel for rainfall determinations compared with the estimation algorithm which performs its rainfall determinations on a 54 x 54 km grid.

The SMMR data indicate the presence of larger scale precipitation events, and this knowledge can be useful in forecasting and analysis. Figure 7 shows that portion of the North American surface map covering the Gulf of Alaska for 18Z, September 18, 1978. Superimposed on this map are areas of precipitation as determined by the SEASAT SMMR using both the estimation and regression algorithms. The map shows a low (or wave) centered just south and west of Ocean Weather Station Papa. Because the front is a cold front, precipitation is more likely to occur behind rather than ahead of the front. The precipitation data suggest that the front should be advanced slightly to south and east. This in turn suggests that the center should be located to the south and west of its depicted position (48°N, 150°W). GOES imagery from this period tends to support this conclusion. In fact, the leading edge of the precipitation coincides with the edge of a band of cold (and therefore presumably) high clouds shown in the GOES infrared imagery.

CONCLUSION AND SUMMARY

The analysis presented in this report supports the conclusion that the SEASAT SMMR gives reliable and accurate estimates of total precipitable water on a global scale. The error statistics, in fact, are quite comparable to those for radiosondes. In the tropics, the SMMR appears to be a reliable indicator of the presence of rain over the ocean. In the midlatitudes (GOASEX and JASIN), the SMMR apparently misses small areas and/or areas of light rain but detects larger scale precipitation events.

*Joint Air Sea Interaction Experiment

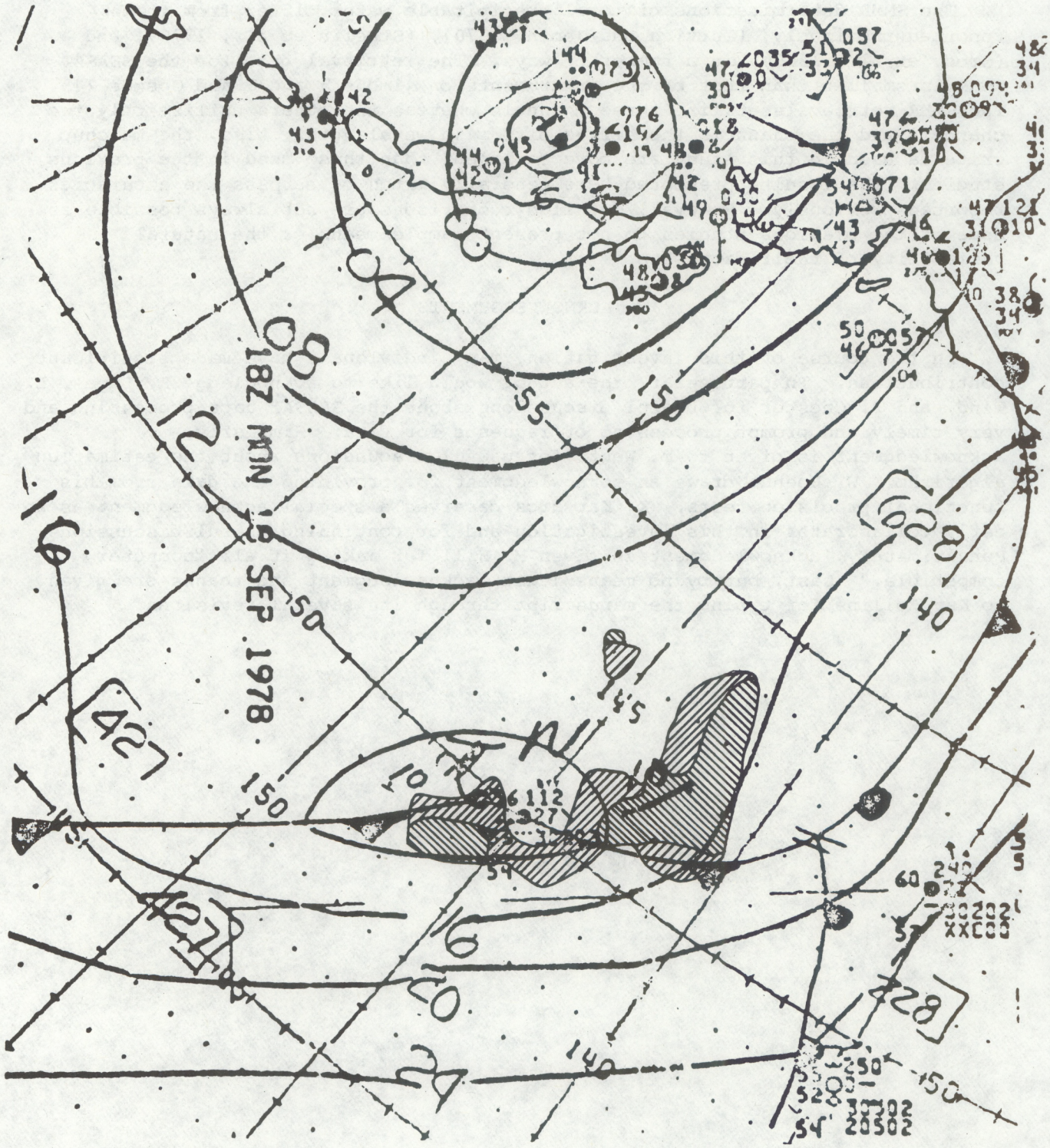

Figure 7.-- 18Z North American NMC surface map for area surrounding Ocean Weather Station Papa. The date is September 18, 1978. The SEASAT overpass (Rev. 1198) occurred at 18:38:37Z. The hatched area with negative slope, as viewed from left to right, is the region of precipitation as determined by the estimation algorithm. The region of precipitation as determined by the regression algorithm comprises both hatched areas.

The SMMR determinations of total precipitable water differ from those reported previously, (Gurvich and Demin, 1970), (Staelin et al., 1976), and (Grody et al., 1980), in a number of ways. The retrieval grid for the SEASAT SMMR is smaller than that of the instruments on Nimbus 5 and 6 and Cosmos 243. The SMMR retrievals utilize three channels whereas the others utilize only two channels and the channels themselves differ in wavelength. Also, the matchup criteria used in this study are more stringent than those used in the previous studies. The results presented here generally match or surpass the accuracies reported previously. However, detailed comparisons are not always possible as some of the previous studies do not present sample means or the natural variability of their data sets.

ACKNOWLEDGEMENTS

In the course of this investigation, many individuals have made significant contributions. In particular, the author would like to acknowledge R. Lipes, B. Wind, and T. Chester for useful discussions about the SEASAT data processing and very timely and prompt processing of requests for data. Similarly, acknowledgment is given to F. Wentz for useful discussions about the estimation algorithm. W. Hoehne draws an acknowledgment for providing the data from his functional precision tests. K. Katsaros deserves a special acknowledgment as an early collaborator in this investigation and for continuing useful discussions. Penultimately, acknowledgment is given M. Hill for making it all "computer compatible." Last, but by no means least, acknowledgment and thanks are given to Kay Collins for typing the manuscript through its several revisions.

References

Bierman, G.J., R.G. Lipes, and F.J. Wentz, 1978: Modern estimation techniques applied to microwave sensing of the marine boundary layer. Proc. Twelfth Asilomar Conference on Circuits, Systems, and Computers (IEEE Computer Society) 101-106.

Born, G.H., J.A. Dunne, and D.B. Lame, 1979: SEASAT mission overview. Science, 204, 1405-1406.

Gloersen, P., and F.T. Barath, 1977: A scanning multichannel microwave radiometer for Nimbus-G and SEASAT-A. IEEE J. Oceanic Eng. OE-2, 172-178.

Grody, N.G., A. Gruber and W. Shen, 1980: Atmospheric water content over the tropical Pacific derived from the Nimbus-G scanning microwave spectrometer. J. Appl. Meteor., 19, 986-996.

Gurvich, A.S. and V.V. Demin, 1970: Determination of the Total moisture content in the atmosphere from measurements on the Cosmos 243 satellite. Atmospheric and Oceanic Physics, 6, 453-457.

Hoehne, W.E., 1980: Precision of national weather service upper air measurements. NOAA Technical Memorandum NWS T&ED-16 NOAA, NWS, Sterling, VA, 23 pp.

Prabhakara, C., H.D. Chang, and A.T.C. Chang, 1981: Remote sensing of precipitable water over the oceans from Nimbus-7 microwave measurements. NASA Technical Memorandum 82117, NASA, GSFC, Greenbelt, MD, 26 pp.

SEASAT, 1979a: SEASAT Gulf of Alaska Workshop (January, 1979) Report. Vol. I and II, JPL Document No. 622-101, NASA JPL, Pasadena, CA.

SEASAT, 1979b: Scanning Multichannel Microwave Radiometer Mini-Workshop I (April, 1979) Report, JPL Document No. 622-208, NASA, JPL, Pasadena, CA., 33 pp.

SEASAT, 1979c: Scanning Multichannel Microwave Radiometer Mini-Workshop II (September, 1979) Report. JPL Document No. 622-212, NASA, JPL, Pasadena, CA., 43 pp.

SEASAT, 1980a: Scanning Multichannel Microwave Radiometer Mini-Workshop III (August, 1980) Report. JPL Document No, 622-224, NASA-JPL, Pasadena, CA., 101 pp.

SEASAT, 1980b: SEASAT-JASIN Workshop Report. Vol. I, JPL Document No. 80-62, NASA-JPL, Pasadena, CA., 397 pp.

SEASAT, 1981: Scanning Multichannel Microwave Radiometer Mini-Workshop IV (April, 1981) Report. JPL Document No. 622-234, NASA-JPL, Pasadena, CA. 129 pp.

Staelin, D.H., K.F. Kunzi, R.L. Pettyjohn, R.K..L. Poon, R.W. Wilcox, and J.W. Waters, 1976: remote sensing of atmospheric water vapor and liquid water with the Nimbus 5 microwave spectrometer. J. Appl. Meteor., 15, 1204-1214.

Tetens, O., 1930: Uber einige meteorologische Begriffe. Z. Geophys., 6, 297-309.

Wentz, F.J., 1982: A model function for ocean microwave brightness temperatures. J. Geophys. Res. (to be published).

Wilheit, T.T., A.T.C. Chang, M.S.V. Rao, E.B. Rodgers, and J.S. Theon, 1977: A satellite technique for quantitatively mapping rainfall rates over the oceans. J. Appl. Meteor., 16, 551-560.

Wilheit, T.T. and A.T.C. Chang, 1979: An algorithm for retrieval of ocean surface and atmospheric parameters from the observations of the scanning multichannel microwave radiometer (SMMR). NASA Technical Memorandum 80277, NASA, GSFC, Greenbelt, MD, 30 pp.

Wilkerson, J.C., R.A. Brown, V.J. cardone, R.E. Coons, A.A. Loomis, J.E. Overland, S. Peteherych, W.J. Pierson, P.M. Woiceshyn, and M.G. Wuertele, 1979: Surface observations for the evaluation of geophysical measurements from SEASAT. Science, 204, 1408-1410.

Appendix A

Radiosonde Corrections and Listing

Using a midlatitude climatological atmosphere with water vapor concentrations from the surface to 0.1 mb as a reference, it was decided that 1) radiosondes for which humidity data were available to at least 300 mb would not need correcting, and 2) radiosondes for which the humidity data did not reach 300 mb, a proportional correction (based on the amount of water vapor in the observed atmosphere and the fraction of the total water vapor in the reference atmosphere) would be used. The exact form of the correction is: $U=U^*(1+ U'/1.334)$, where U = total precipitable water, U^* = amount of water vapor calculated from the radiosonde, U' = amount of water vapor in the reference atmosphere above the pressure level of the radiosonde, and 1.334 gm/cm^2 = total precipitable water in the reference atmosphere. For Ocean Station PAPA U' = 0.03 gm/cm^2 in all cases. Table A1 gives the various parameters for the R/V Oceanographer radiosondes. In Table A1 $\Delta U=U^*U'/1.334$, so that $U=U^*+\Delta U$. Table A2 gives the total precipitable water amounts from Ocean Station Papa. These are the corrected amounts. Table A3 lists the total precipitable water amounts from the tropical island stations and Ocean Station Tango.

Table A1. - Oceanographer raobs and corrections

Date	Height (mb)	U*(gm/cm^2)	U'	ΔU	U	Rev.	Time
8/31	303	1.75	0	0	1.75	940	1737
9/01	424	1.65	.03	.04	1.69	949	0840
9/01	735	1.34	.32	.32	1.66	954	1655
9/06	411	3.53	.03	.08	3.61	1025	1553
9/07	318	1.46	0	0	1.46	1034	0707
9/07	216	1.54	0	0	1.54	1040	1728
9/08	439	1.92	.03	.04	1.96	1054	1713
9/09	539	1.48	.08	.09	1.57	1063	0753
9/09	416	1.47	.03	.03	1.50	1069	1748
9/10	441	2.41	.03	.05	2.46	1077	0806
9/10	370	2.72	.02	.04	2.76	1083	1729
9/11	473	2.33	.04	.07	2.40	1092	0909
9/12	735	1.24	.32	.30	1.54	1106	0840
9/13	329	1.61	.01	.01	1.62	1120	0747
9/13	430	1.93	.03	.04	1.97	1126	1727
9/14	672	1.45	.25	.27	1.72	1135	0904
9/14	478	1.35	.04	.04	1.37	1140	1756
9/15	588	1.21	.14	.13	1.34	1149	0837
9/15	454	1.82	.04	.05	1.87	1155	1814
9/16	493	1.17	.06	.05	1.22	1163	0819
9/16	428	1.23	.03	.03	1.26	1169	1756
9/17	573	1.64	.13	.16	1.80	1183	1727
9/18	403	3.31	.03	.07	3.38	1192	0933
9/20	478	1.36	.04	.04	1.40	1221	0927
9/20	553	1.43	.09	.10	1.53	1226	1732
9/22	538	1.19	.08	.07	1.26	1249	0833
9/22	670	1.45	.25	.27	1.72	1255	1822
9/23	639	1.19	.21	.19	1.38	1263	0845
9/23	381	1.68	.02	.03	1.71	1269	1753
9/24	463	2.16	.04	.06	2.22	1278	0917
9/24	384	2.51	.02	.04	2.55	1283	1725
9/25	368	2.16	.02	.03	2.19	1292	0914
9/25	787	1.66	.42	.52	2.18	1298	1845

TABLE A2. - Papa raobs

Date	Time (Z)	H_2O amount (gm/cm^2)	Rev
July 16	0440	2.1	274
July 17	0711	3.7	
July 17	1353	3.1	294
July 19	0449	2.2	317
July 20	0856	1.7	
July 20	1400	1.5	337
July 22	0456	1.8	360
July 23	0903	2.6	
July 23	1407	2.4	380
July 25	0503	2.5	403
July 26	0610	1.7	
July 26	1414	1.9	423
July 28	0511	2.7	446
July 29	0618	2.2	461
July 29	1421	2.1	
July 31	0517	2.1	
July 31	1500	2.2	495
August 1	0625	2.5	
August 1	1427	2.0	
August 3	0702	1.9	
August 4	0632	1.7	
August 4	1436	1.6	
August 6	0709	3.9	
August 7	0639	3.0	590
August 7	1443	2.3	
August 9	0716	1.7	619
August 10	0646	2.7	633
August 10	1450	2.0	
August 12	0723	3.0	
August 13	0653	3.2	676
August 13	1636	2.9	
August 15	0730	1.4	
August 16	0700	2.5	719
August 16	1643	2.6	725
August 18	0738	2.5	
August 19	0708	2.5	762
August 19	1650	2.2	768
August 21	0745	1.4	
August 22	0715	2.8	805
August 22	1657	2.7	811
August 24	0752	1.2	834
August 25	0722	1.7	848
August 25	1704	2.2	854
August 27	0759	2.6	877

Table A2. - Papa Raobs (continued)

DATE	TIME (Z)	H_2O AMOUNT (gm/cm^2)	REV
August 28	0729	2.8	891
August 28	1711	1.9	987
August 30	0806	1.5	920
August 31	0736	1.8	934
August 31	1719	1.9	940
September 2	0820	1.6	963
September 3	0752	1.4	977
September 3	1735	1.6	983
September 5	0832	2.9	1006
September 6	0804	3.7	1020
September 6	1748	1.2	1026
September 8	0846	2.0	1049
September 12	0830	1.8	1106
September 14	0911	1.2	1135
September 15	0842	1.2	1149
September 15	1825	1.4	1155
September 17	0923	1.3	1178
September 18	0854	2.6	1192
September 18	1938	3.5	1198
September 19	1809	1.8	1212
September 20	0936	1.6	1221
September 21	0907	1.4	1235
September 21	1851	1.1	1241
September 22	1821	1.2	1255
September 23	0948	1.2	1264
September 24	0921	1.1	1278
September 24	1903	1.3	1284
September 25	1834	1.2	1298
September 26	1001	2.5	1307
September 30	1923	2.1	1370
October 3	1941	2.3	1413
October 6	1956	1.4	1456
October 9	2007	1.0	1499

Table A3. - Tropical raobs

Station	Date	Time (Z)	H_2O amount (gm/cm^2)	Rev
Fiji	10 Sep	2300	3.9	1085-6
Fiji	13 Sep	2300	2.0	1128-9
Fiji	16 Sep	2300	2.6	1171-2
Fiji	25 Sep	2300	3.9	1300-1
Fiji	28 Sep	2300	2.3	1343-4
Fiji	1 Oct	2300	3.6	1386-7
Fiji	2 Oct	2300	5.4	-
Funafuti	10 Sep	2300	4.7	1085-6
Funafuti	13 Sep	2300	3.8	1128-9
Funafuti	16 Sep	2300	3.2	1171-2
Funafuti	19 Sep	2300	3.7	1214-5
Funafuti	22 Sep	2300	6.4	1257-8
Funafuti	25 Sep	2300	5.1	1300-1
Funafuti	28 Sep	2300	5.4	1343-4
Funafuti	1 Oct	2300	6.3	1386-7
Funafuti	2 Oct	2300	6.1	-
Guam	10 Sep	2304	5.6	1087
Guam	13 Sep	2300	5.4	1130
Guam	16 Sep	2300	5.0	1173
Guam	19 Sep	2300	5.1	1216
Guam	22 Sep	2300	5.9	1259
Guam	26 Sep	0007	5.0	1302
Guam	28 Sep	2300	6.0	1345
Guam	1 Oct	2300	5.2	1388
Honiara	2 Oct	2300	4.0	1401
Johnston Is.	13 Sep	2315	5.3	1135
Johnston Is.	14 Sep	1115	4.7	1135
Johnston Is.	16 Sep	2315	5.4	1178
Johnston Is.	17 Sep	1115	4.8	1178
Kwajalein	10 Sep	2300	5.5	1085-6
Kwajalein	13 Sep	2030	5.6	1128-9
Kwajalein	15 Sep	2300	5.8	1158
Kwajalein	16 Sep	2300	5.1	1171-2
Kwajalein	18 Sep	2300	5.8	1201
Kwajalein	19 Sep	1100	6.2	-
Kwajalein	19 Sep	2300	6.6	1214-5

Table A3. - Tropical raobs (continued)

Station	Date	Time (Z)	H_2O amount (gm/cm^2)	Rev
Kwajalein	22 Sep	1943	6.3	1257-8
Kwajalein	24 Sep	2300	5.2	1287
Kwajalein	25 Sep	1928	5.6	1300-1
Kwajalein	26 Sep	2300	5.6	-
Kwajalein	28 Sep	2300	5.0	1343-4
Kwajalein	1 Oct	2300	5.3	1386-7
Majuro	9 Sep	0	6.2	1064
Majuro	10 Sep	2255	4.5	-
Majuro	12 Sep	2235	5.2	-
Majuro	13 Sep	2255	6.2	1128-9
Majuro	15 Sep	2235	5.7	-
Majuro	16 Sep	2245	6.1	1171-2
Majuro	18 Sep	2328	5.8	-
Majuro	19 Sep	2255	5.0	1214-5
Majuro	21 Sep	2255	5.8	-
Majuro	24 Sep	2320	5.4	-
Majuro	25 Sep	2250	5.2	1300-1
Majuro	26 Sep	2320	5.3	-
Majuro	28 Sep	2255	5.5	1343-4
Majuro	1 Oct	2255	4.6	1386-7
Noumea	2 Oct	2300	1.8	1401
Ponape	11 Sep	2255	4.9	1101
Ponape	14 Sep	2257	6.0	1144
Ponape	17 Sep	2302	5.6	1187
Ponape	20 Sep	2314	5.3	1230
Ponape	23 Sep	2256	5.2	1273
Ponape	26 Sep	2359	5.7	1316
Ponape	29 Sep	2304	5.5	1359
Ponape	2 Oct	2317	5.8	1402
Tango	11 Sep	0	5.8	1087
Tango	14 Sep	0	5.0	1130
Tango	17 Sep	0	4.7	1173
Tango	20 Sep	0	6.3	1216
Tango	23 Sep	0	5.8	1259
Tango	26 Sep	0	3.5	1302
Tango	29 Sep	0	4.1	1345
Tango	2 Oct	0	3.5	1388

Table A3. - Tropical raobs (continued)

Station	Date	Time (Z)	H_2O amount (gm/cm^2)	Rev
Truk	11 Sep	2255	5.3	1101
Truk	14 Sep	2255	6.0	1144
Truk	17 Sep	2255	5.6	1187
Truk	20 Sep	2255	4.8	1230
Truk	23 Sep	2257	6.3	1273
Truk	26 Sep	2255	5.1	1316
Truk	29 Sep	2255	6.4	1359
Truk	2 Oct	2255	5.9	1402
Vila	3 Oct	0	3.5	1401
Wake Is.	9 Sep	0	5.5	-
Wake Is.	9 Sep	12	4.8	-
Wake Is.	10 Sep	2300	5.0	1085-6
Wake Is.	13 Sep	2300	5.3	1128-9
Wake Is.	16 Sep	2300	3.6	1171-2
Wake Is.	19 Sep	2300	4.2	1214-5
Wake Is.	28 Sep	2300	5.5	1343-4
Wake Is.	1 Oct	2300	4.7	1386-7

Appendix B

Programs to Compute Total Precipitable Water

```
C     THE PURPOSE OF THIS PROGRAM IS TO INPUT RADIOSONDE PRESSURE,
C TEMPERATURE, AND DEWPOINT DEPRESSION AND COMPUTE THE TOTAL
C PRECIPITABLE WATER AMOUNT.
C
C CGRAV = THE CONSTANT OF GRAVITY.
C DPD = DEWPOINT DEPRESSION.
C P = PRESSURE (MB).
C T = TEMPERATURE (DEGREES C).
C WVMR = WATER VAPOR MIXING RATIO (G/KG).
C
      DIMENSION HEADER(20),P(99),T(99),DPD(99),WVMR(99)
C
      CGRAV=980.665
  100 READ (5,6000,END=900) HEADER
 6000 FORMAT (20A4)
      PRINT 6010,HEADER
 6010 FORMAT (1H1,20A4,/)
      PRINT 6050
 6050 FORMAT (1H ,3X,'P',7X,'T',6X,'DPD',3X,'WVMR')
      J=1
  150 READ 6020,P(J),T(J),DPD(J)
 6020 FORMAT (F6.1,1X,F5.1,1X,F4.1)
      IF (P(J) .EQ. 9999.9) GO TO 180
      J=J+1
      IF (J .LE. 99) GO TO 150
   99 STOP 99
  180 NUMLEV=J-1
C CONVERT DEWPOINT DEPRESSION TO MIXING RATIO (G/KG).
      DO 240 J=1,NUMLEV
      DEWPTT=T(J)-DPD(J)
      E1=6.11*EXP((17.27*DEWPTT)/(237.3+DEWPTT))
      WVMR(J)=(621.98*E1)/(P(J)-E1)
      PRINT 6030,P(J),T(J),DPD(J),WVMR(J)
 6030 FORMAT (1H ,F6.1,3X,F5.1,3X,F4.1,3X,F4.1)
  240 CONTINUE
C COMPUTE TOTAL PRECIPITABLE WATER.
      TOTH2O=0.0
      DO 300 J=2,NUMLEV
      TOTH2O=TOTH2O +
     1   (P(J-1)-P(J))*((WVMR(J-1)+WVMR(J))/2.0)/CGRAV
  300 CONTINUE
      PRINT 6040,TOTH2O
 6040 FORMAT (//,1H ,'TOTAL PRECIPITABLE WATER IS ',F5.2)
      GO TO 100
C
  900 STOP 1
      END
```

```
C     THE PURPOSE OF THIS PROGRAM IS TO INPUT RADIOSONDE PRESSURE,
C TEMPERATURE, AND RELATIVE HUMIDITY AND COMPUTE THE TOTAL
C PRECIPITABLE WATER AMOUNT.
C
C CGRAV = THE CONSTANT OF GRAVITY.
C P = PRESSURE (MB).
C RH = RELATIVE HUMIDITY (PERCENT).
C T = TEMPERATURE (DEGREES C).
C WVMR = WATER VAPOR MIXING RATIO (G/KG).
C
      DIMENSION HEADER(20),P(99),T(99),RH(99),WVMR(99)
C
      CGRAV=980.665
  100 READ (5,6000,END=900) HEADER
 6000 FORMAT (20A4)
      PRINT 6010,HEADER
 6010 FORMAT (1H1,20A4,/)
      PRINT 6050
 6050 FORMAT (1H ,3X,'P',7X,'T',6X,'RH',4X,'WVMR')
      J=1
  150 READ 6020,P(J),T(J),RH(J)
 6020 FORMAT (F6.1,1X,F5.1,1X,F2.0)
      IF (P(J) .EQ. 9999.9) GO TO 180
      J=J+1
      IF (J .LE. 99) GO TO 150
   99 STOP 99
  180 NUMLEV=J-1
C CONVERT RELATIVE HUMIDITY TO MIXING RATIO (G/KG).
      DO 240 J=1,NUMLEV
      EW=6.11*EXP((17.27*T(J))/(237.3+T(J)))
      EI=EW*RH(J)/100.0
      WVMR(J)=(621.98*EI)/(P(J)-EI)
      PRINT 6030,P(J),T(J),RH(J),WVMR(J)
 6030 FORMAT (1H ,F6.1,3X,F5.1,3X,F4.1,3X,F4.1)
  240 CONTINUE
C COMPUTE TOTAL PRECIPITABLE WATER.
      TOTH2O=0.0
      DO 300 J=2,NUMLEV
      TOTH2O=TOTH2O +
     1   (P(J-1)-P(J))*((WVMR(J-1)+WVMR(J))/2.0)/CGRAV
  300 CONTINUE
      PRINT 6040,TOTH2O
 6040 FORMAT (//,1H ,'TOTAL PRECIPITABLE WATER IS ',F5.2)
      GO TO 100
C
  900 STOP 1
      END
```

Appendix C

Radiosonde Total Precipitable Water Precision

Radiosonde observations (raobs) are the main source of surface observations of total precipitable water for comparison with satellite determinations. An important factor in comparisons of this type is the intrinsic accuracy of the raobs. Recent work (Hoehne, 1980) permits the answering of some of the questions about the precision of raob determination of total precipitable water. Between April 5, 1978, and May 22, 1979, a series of 50 ascensions were made from Dulles International Airport with two identical sondes on the same balloon. The sondes were separated by a distance of about five meters. A tape of the actual radiosonde values of pressure, temperature, and dew point depression was obtained and the amount of total precipitable water was calculated. Four of the ascensions were eliminated from the data set. The operational sonde was the lower sonde in the train in all cases. Table C1 gives the statistics for this study.

Table C1. - Raob precision statistics

mean of op. sonds = 2.03 gm/cm^2 n = 46

bias = op. sonde - test sonde = 0.04 gm/cm^2

$$\text{mean square difference} = \left\{ \frac{\Sigma[1 \text{ op. sonde})_i - (\text{test sonde})_i]^2}{n} \right\}^{\frac{1}{2}} = 0.13 \text{ gm/cm}^2$$

m.s.d. with bias removed = 0.12 gm/cm^2

variance for one radiosonde = 0.085 gm/cm^2

coefficient of variance = 0.085/2.03 = 0.042

The small bias between the operational and test sondes is caused by the water actuated batteries of the test sonde. This battery pack is located between the test and operational sondes. The statistical significance can be inferred by performing a chi-squared test on the signs of the difference, Δ = op. sonde-test sonde. There were 32 positive differences and only 14 negative differences. Thus $\chi^2 = 7.04$. Figure C1 is an error histogram for the differences. The solid lines indicate the observed values and the dashed lines the expected. The increments are 0.1 gm/cm^2. As can be seen from the figure and the value of chi-squared, the difference statistics are well described by a normal distribution. The complete raob data set is presented in Table C2.

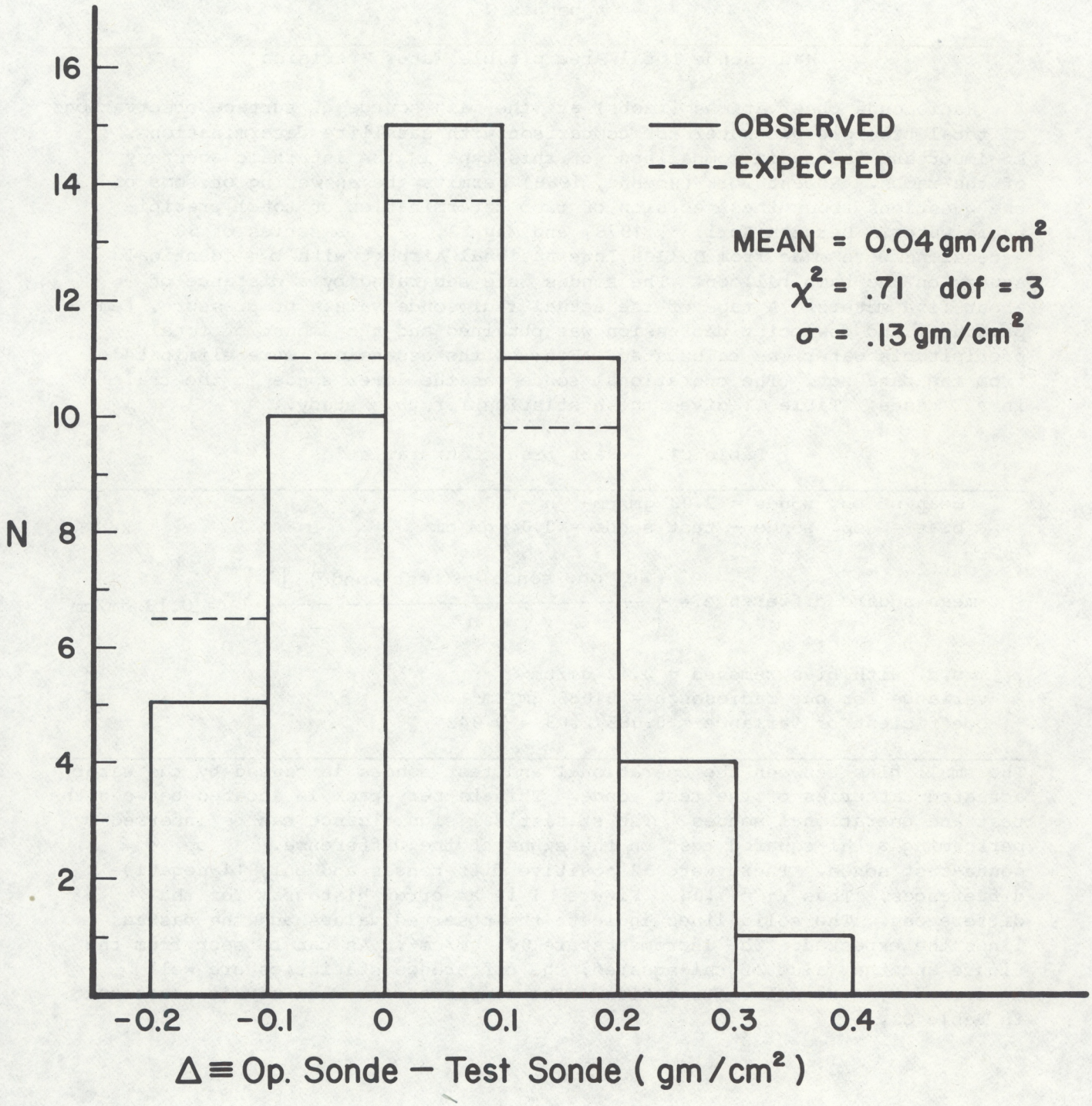

Figure C1.-- Error histogram for the raob comparison. The abscissa shows the difference between the operational and test sondes. The ordinate shows the number of differences in each 0.1 gm/cm^2 interval.

Table C2

Date	Flight	Test sonde	Op sonde
4/05/78	1	1.82	1.63
5/19/78	2	1.97	2.13
5/25/78	3	2.47	2.50
6/01/78	4	1.88	2.11
6/08/78	5	4.55	4.70
6/15/78	6	1.78	1.89
6/29/78	8	2.84	3.02
7/06/78	9	1.86	1.90
7/13/78	10	1.63	1.49
7/20/78	11	2.64	2.83
7/25/78	12	4.49	4.32
8/03/78	13	4.62	4.72
8/16/78	14	3.51	3.66
8/30/78	16	4.40	4.61
9/07/78	17	2.14	2.35
9/14/78	18	2.86	2.96
9/21/78	19	3.62	3.72
9/28/78	20	2.22	2.13
10/04/78	21	2.73	2.90
10/12/78	22	2.01	2.38
10/24/78	24	0.54	0.50
11/02/78	25	0.51	0.58
11/09/78	26	0.82	0.85
11/16/78	27	2.68	2.91
11/23/78	28	1.27	1.22
11/30/78	29	0.94	0.94
12/06/78	30	0.94	1.13
12/13/78	31	0.68	0.72
13/20/78	32	2.96	2.76
1/04/79	33	0.30	0.37
1/10/79	34	0.66	0.64
1/17/79	35	1.06	1.06
2/06/79	37	0.46	0.42
2/14/79	38	1.24	1.28
3/07/79	39	0.62	0.62
3/14/79	40	0.56	0.56
3/21/79	41	1.07	1.13
3/29/79	42	2.31	2.15
4/04/79	43	2.28	2.22
4/11/79	44	2.00	2.02
4/18/79	45	0.98	0.94
4/25/79	46	2.95	3.01
5/01/79	47	0.70	0.63
5/09/79	48	2.68	2.75
5/15/79	49	0.90	0.84
5/22/79	50	3.15	3.14

(Continued from inside front cover)

NESS 61 The Measurement of Atmospheric Transmittance From Sun and Sky With an Infrared Vertical Sounder. W. L. Smith and H. B. Howell, September 1972, 16 pp. (COM-73-50020)

NESS 62 Proposed Calibration Target for the Visible Channel of a Satellite Radiometer. K. L. Coulson and H. Jacobowitz, October 1972, 27 pp. (COM-73-10143)

NESS 63 Verification of Operational SIRS B Temperature Retrievals. Harold J. Brodrick and Christopher M. Hayden, December 1972, 26 pp. (COM-73-50279)

NESS 64 Radiometric Techniques for Observing the Atmosphere From Aircraft. William L. Smith and Warren J. Jacob, January 1973, 12 pp. (COM-73-50376)

NESS 65 Satellite Infrared Soundings From NOAA Spacecraft. L. M. McMillin, D. Q. Wark, J.M. Siomkajlo, P. G. Abel, A. Werbowetzki, L. A. Lauritson, J. A. Pritchard, D. S. Crosby, H. M. Woolf, R. C. Luebbe, M. P. Weinreb, H. E. Fleming, F. E. Bittner, and C. M. Hayden, September 1973, 112 pp. (COM-73-50936/6AS)

NESS 66 Effects of Aerosols on the Determination of the Temperature of the Earth's Surface From Radiance Measurements at 11.2 m. H. Jacobowitz and K. L. Coulson, September 1973, 18 pp. (COM-74-50013)

NESS 67 Vertical Resolution of Temperature Profiles for High Resolution Infrared Radiation Sounder (HIRS). Y. M. Chen, H. M. Woolf, and W. L. Smith, January 1974, 14 pp. (COM-74-50230)

NESS 68 Dependence of Antenna Temperature on the Polarization of Emitted Radiation for a Scanning Microwave Radiometer. Norman C. Grody, January 1974, 11 pp. (COM-74-50431/AS)

NESS 69 An Evaluation of May 1971 Satellite-Derived Sea Surface Temperatures for the Southern Hemisphere. P. Krishna Rao, April 1974, 13 pp. (COM-74-50643/AS)

NESS 70 Compatibility of Low-Cloud Vectors and Rawins for Synoptic Scale Analysis. L. F. Hubert and L. F. Whitney, Jr., October 1974, 26 pp. (COM-75-50065/AS)

NESS 71 An Intercomparison of Meteorological Parameters Derived From Radiosonde and Satellite Vertical Temperature Cross Sections. W. L. Smith and H. M. Woolf, November 1974, 13 pp. (COM-75-10432)

NESS 72 An Intercomparison of Radiosonde and Satellite-Derived Cross Sections During the AMTEX. W. C. Shen, W. L. Smith, and H. M. Woolf, February 1975, 18 pp. (COM-75-10439/AS)

NESS 73 Evaluation of a Balanced 300-mb Height Analysis as a Reference Level for Satellite-Derived soundings. Albert Thomasell, Jr., December 1975, 25 pp. (PB-253-058)

NESS 74 On the Estimation of Areal Windspeed Distribution in Tropical Cyclones With the Use of Satellite Data. Andrew Timchalk, August 1976, 41 pp. (PB-261-971)

NESS 75 Guide for Designing RF Ground Receiving Stations for TIROS-N. John R. Schneider, December 1976, 126 pp. (PB-262-931)

NESS 76 Determination of the Earth-Atmosphere Radiation Budget from NOAA Satellite Data. Arnold Gruber, November 1977, 31 pp. (PB-279-633)

NESS 77 Wind Analysis by Conditional Relaxation. Albert Thomasell, Jr., January 1979.

NESS 78 Geostationary Operational Environmental Satellite/Data Collection System. July 1979, 86 pp. (PB-301-276)

NESS 79 Error Characteristics of Satellite-Derived Winds. Lester F. Hubert and Albert Thomasell, Jr. June 1979, 44 pp. (PB-300-754)

NESS 80 Calculation of Atmospheric Radiances and Brightness Temperatures in Infrared Window Channels of Satellite Radiometers. Michael P. Weinreb and Michael L. Hill, March 1980, 43 pp. (PB80 208-119)

NESS 81 Improved Algorithm for Calculation of UTM and Geodetic Coordinates. Jeff Dozier, September 1980, 21 pp. (PB81 132680)

NESS 82 The Effect of Precipitation on Microwave Soundings in Low Latitudes. Lester F. Hubert, Norman C. Grody, Andrew Timchalk, and William C. Shen, April 1981, 34 pp. (PB81 225062)

NESS 83 Atmospheric Sounding User's Guide. Adolf Werbowetzki, ed., April 1981, 82 pp. (PB81 230476)

NESS 84 Use of NOAA/AVHRR Visible and Near-Infrared Data for Land Remote Sensing. Stanley R. Schneider, David F. McGinnis Jr., James A. Gatlin, September 1981. (PB82 129388)

NESS 85 Transmittances for the TIROS Operational Vertical Sounder. M.P. Weinreb, H.E. Fleming, L.M. McMillin, and A.C. Neuendorffer, September 1981. (PB82 155920)

NESS 86 Statistical and Synoptic Evaluations of TIROS-N and NOAA-6 Retrievals. Harold J. Brodrick, Carmella Watkins, and Arnold Gruber, October 1981. (PB82 188053)

NESS 87 Satellite Observations of Variations in Northern Hemisphere Seasonal Snow Cover. Kenneth F. Dewey and Richard Heim, Jr. December 1981. (PB82 196668)

NESS 88 Observations of Hurricane David (1979) Using the Microwave Sounding Unit. Norman C. Grody and William C. Shen, March 1982.

NESS 89 A Statistical Approach to Rainfall Estimation Using Satellite and Conventional Data. Linwood F. Whitney, Jr. April 1982, 50 pp.

NOAA SCIENTIFIC AND TECHNICAL PUBLICATIONS

The National Oceanic and Atmospheric Administration was established as part of the Department of Commerce on October 3, 1970. The mission responsibilities of NOAA are to assess the socioeconomic impact of natural and technological changes in the environment and to monitor and predict the state of the solid Earth, the oceans and their living resources, the atmosphere, and the space environment of the Earth.

The major components of NOAA regularly produce various types of scientific and technical information in the following kinds of publications:

PROFESSIONAL PAPERS — Important definitive research results, major techniques, and special investigations.

CONTRACT AND GRANT REPORTS — Reports prepared by contractors or grantees under NOAA sponsorship.

ATLAS — Presentation of analyzed data generally in the form of maps showing distribution of rainfall, chemical and physical conditions of oceans and atmosphere, distribution of fishes and marine mammals, ionospheric conditions, etc.

TECHNICAL SERVICE PUBLICATIONS — Reports containing data, observations, instructions, etc. A partial listing includes data serials; prediction and outlook periodicals; technical manuals, training papers, planning reports, and information serials; and miscellaneous technical publications.

TECHNICAL REPORTS — Journal quality with extensive details, mathematical developments, or data listings.

TECHNICAL MEMORANDUMS — Reports of preliminary, partial, or negative research or technology results, interim instructions, and the like.

Information on availability of NOAA publications can be obtained from:

ENVIRONMENTAL SCIENCE INFORMATION CENTER (OA/D812)
ENVIRONMENTAL DATA AND INFORMATION SERVICE
NATIONAL OCEANIC AND ATMOSPHERIC ADMINISTRATION
U.S. DEPARTMENT OF COMMERCE
Rockville, MD 20852

NOAA--S/T 82-90